Biochimica et Biophysica Acta 1837 (2014) 1998–2003

Contents lists available at ScienceDirect

Biochimica et Biophysica Acta

journal homepage: www.elsevier.com/locate/bbabio

Lysine 362 in cytochrome *c* oxidase regulates opening of the K-channel via changes in pK_A and conformation

Anna Lena Woelke, Gegham Galstyan, Ernst-Walter Knapp *

Institute of Chemistry and Biochemistry, Freie Universität Berlin, D-14195 Berlin, Germany

ARTICLE INFO

Article history:
Received 12 June 2014
Received in revised form 9 August 2014
Accepted 12 August 2014
Available online 19 August 2014

Keywords:
Cytochrome *c* oxidase
K-channel
Proton transfer path
Electrostatics
Metabolism

ABSTRACT

The metabolism of aerobic life uses the conversion of molecular oxygen to water as an energy source. This reaction is catalyzed by cytochrome *c* oxidase (C*c*O) consuming four electrons and four protons, which move along specific routes. While all four electrons are transferred via the same cofactors to the binuclear reaction center (BNC), the protons take two different routes in the A-type C*c*O, i.e., two of the four chemical protons consumed in the reaction arrive via the D-channel in the oxidative first half starting after oxygen binding. The other two chemical protons enter via the K-channel in the reductive second half of the reaction cycle. To date, the mechanism behind these separate proton transport pathways has not been understood.
In this study, we propose a model that can explain the reaction-step specific opening and closing of the K-channel by conformational and pK_A changes of its central lysine 362. Molecular dynamics simulations reveal an upward movement of Lys362 towards the BNC, which had already been supposed by several experimental studies. Redox state-dependent pK_A calculations provide evidence that Lys362 may protonate transiently, thereby opening the K-channel only in the reductive second half of the reaction cycle. From our results, we develop a model that assigns a key role to Lys362 in the proton gating between the two proton input channels of the A-type C*c*O.

1. Introduction

Cytochrome *c* oxidase (C*c*O) is the terminal enzyme in the electron transfer sequence of the respiratory chain of eukaryotes and is also an essential enzyme of many bacteria. In a stepwise reaction, it reduces molecular oxygen to water. The resultant energy is spent to pump protons across the membrane that C*c*O resides in. In the C*c*O reaction cycle, electrons are taken up from soluble cytochrome *c* at the positively charged P-side of the membrane. They are transported via the bimetallic copper A center (Cu_A) to heme *a* and finally to the binuclear center (BNC), where the chemical reaction takes place. The BNC is composed of heme a_3 and copper B (Cu_B). The protons required for C*c*O function are taken up from the negatively charged N-side of the membrane. They can be differentiated into chemical protons consumed in the reaction and pumped protons, which are transported across the membrane. Starting from the N-side, the protons are conducted via two different pathways in the A-type C*c*O—the D-channel originating at D132 and the K-channel containing K362 (residue numbering according to *R. sphaeroides*). It is well established that all pumped protons are taken up via the D-channel, while two chemical protons enter via the D-channel and two via the K-channel. For reviews, see [1,2].

After binding and splitting of molecular oxygen (A → P_M in Fig. 1), the reaction proceeds with the uptake of one electron, one chemical and one pumped proton in each of the four individual reaction steps, which lead to the reduced BNC (state R) that may bind a new oxygen molecule. For the chemical structure inside the BNC, we fully agree with the current view of Wikström and coworkers [1,3,5], except that we added an intermediate state in the P_M → F transition (P → F state in Fig. 1). The chemical structure of the P_R state is presumably only observed in the oxygen-splitting reaction of the fully reduced C*c*O having two additional electrons [4]. Under physiological conditions, the corresponding intermediate state may differ. Nevertheless, both possibilities are investigated and discussed in this study.

The D-channel conducts protons in the oxidative first half of the reaction, while the K-channel operates in the reductive half [6–9]. The reaction is strongly exergonic in the oxidative but only weakly exergonic in the reductive second half of the catalytic cycle, which was suggested as cause for having two separate channels [10]. However, the exact reason for the separate operation of the two proton channels and their mechanisms is a matter of debate. Sharpe and Ferguson-Miller [11] have suggested that a gating mechanism at the end of the K-channel—at Tyr288 and the farnesyl of heme a_3—may be responsible for opening and closing this route. The D-channel that also conducts the pumped protons in every reaction step is filled with an H-bond connected water chain in the crystal structure [12,13]. To close the D-channel during the catalytic

Abbreviations: BNC, binuclear reaction center; Cu_A/Cu_B, copper A/B center; C*c*O, cytochrome *c* oxidase; Glu, glutamate; Lys, lysine; MD, molecular dynamics; PDB, Protein Data Bank; P-side, positive side of the membrane; N-side, negative side of the membrane

* Corresponding author. Tel.: +49 30 838 54 387.
E-mail address: knapp@chemie.fu-berlin.de (E.-W. Knapp).

http://dx.doi.org/10.1016/j.bbabio.2014.08.003
0005-2728/

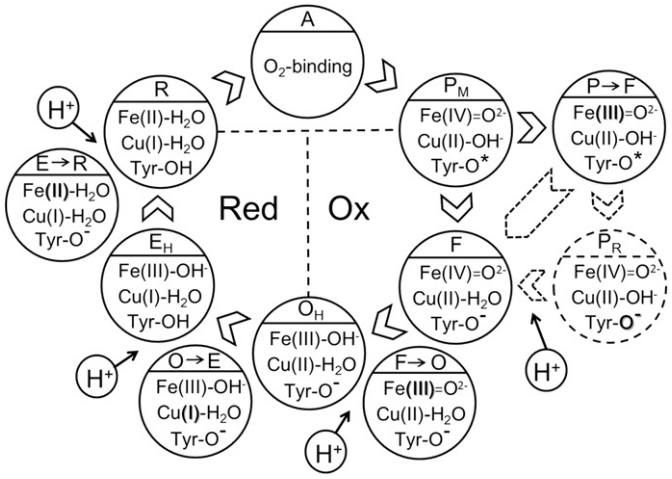

Fig. 1. Catalytic cycle of CcO. In the oxidative first half (Ox) of the cycle, chemical protons are provided by the D-channel, while in the reductive second half (Red), the K-channel transports the chemical protons. Proton (H^+) uptake is indicated by arrows. Redox states are taken from [3], except the P → F intermediate state, which is hypothesized and discussed in the main text. The states depicted outside of the inner cycle denote intermediate states where a new electron has arrived at the BNC. Its location is indicated in bold. The dashed circle denotes state P_R, which is observed under non-physiological, highly reduced conditions [4] (see discussion in text).

cycle, the H-bond chain would need to be disrupted. This would presumably also hinder the transport of pumped protons. However, the opposite is observed: several CcO mutants are incapable of proton-pumping but are still conducting chemical protons [14,15]. In contrast, the K-channel does not exhibit a fully connected water network. In all crystal structures, the conserved lysine (Lys362) points toward the N-side without connecting to the BNC [16,17]. Another exceptional feature of Lys362 is its pK_A value, which is likely strongly downshifted due to the hydrophobic environment. Indeed, several continuum electrostatic calculations predict Lys362 to be deprotonated [18,19], although Tuukkanen et al. [20] suggested a protonated Lys362 considering an explicit water molecule nearby.

Experimental studies gave an indication of the role of the K-channel and the properties of Lys362. The K-channel provides the chemical protons in the reductive second half of the CcO reaction [6–9], where the R → E transition is much faster than the E → O transition [21]. In the reductive phase of the reaction cycle, the first electron may enter the BNC even if the K-channel is blocked by the Lys362Met mutant [22]. Within this phase, proton delivery to the BNC becomes rate-limiting at pH 9.75 [23]. Lys362 also seems to play a role in P_R state formation [24–26]. The P_R state (Fig. 1, dashed cycle) forms after CO release from the fully reduced CcO and its BNC carries one electron more than in the P_M state. It was suggested that in the P_R state, Lys362 may protonate and move towards the BNC to compensate the additional negative charge at the BNC [24–26]. This was concluded from the fact that in K-channel mutants, P_R state formation was slowed down. The slowing down was connected with absorbance changes at 590 nm, which did not show the fast time phase of 60 μs for the K-channel mutants [24]. Monitoring the time evolution of the membrane potential at high pH, an analogue fast phase could not be observed in the K-channel mutants [26]. Hofacker and Schulten [27] noticed that the protonated Lys362 moved towards the BNC in a molecular dynamics (MD) simulation, but did not analyze this finding further. Olkhova et al. [28] observed this movement of Lys362 even in a deprotonated state. On the other hand, in a later 3 ns MD simulation of CcO, the protonated Lys362 did not move toward the BNC [29]. These discrepancies may however be related to differences in the force fields and in the BNC charge models. It is known that protein structures are strongly influenced by electrostatic interactions [30].

In this work, we analyze the redox-dependent flipping behavior of Lys362 with MD simulations and its pK_A value variation during the catalytic cycle of CcO. Our results show a strong correlation between conformational change, pK_A increase of Lys362 and the electron location in the reductive half of the catalytic CcO cycle, where the K-channel delivers the chemical protons. From these results, we deduce a model for the opening and closing mechanism of the K-channel, which can interpret experimental facts that have thus far remained unexplained. Similarly to Glu286, which is a key residue in gating between pumped and chemical protons [12,31], our model assigns a key role to Lys362 in the proton gating between the two proton input channels of CcO.

2. Methods

2.1. Preparing and performing MD simulations of CcO

The coordinates of subunits I and II of CcO from *R. sphaeroides* were taken from the Protein Data Bank [32] [PDB code 2GSM [17]]. Native CcO from *R. sphaeroides* is composed of four subunits, but the smaller enzyme involving only subunits I and II (see Fig. S1 of Supporting Information) is catalytically also active, albeit more vulnerable to high pH values [33]. Subunit III was proposed to function as support of rapid proton uptake via the D-channel [33]. The K-channel, which is more than 20 Å away from subunits III and IV (see Fig. S1 of Supporting Information), is likely not significantly affected by the removal of these subunits. Therefore, only subunits I and II were used for our computations.

The two-subunit CcO protein complex is embedded in a lipid bilayer of phosphatidylcholines modeled with the plug-in of VMD [34] and solvated in a TIP3P [35] water box with periodic boundary conditions. The same setup of MD simulation was used previously [12] employing the CHARMM22 force field [36], CHARMM36 extension for lipids [37] and in-house determined parameters for the cofactors [12]. MD simulations utilized the software NAMD [38], with 2 fs time step using shake to fix the bond lengths involving hydrogen atoms and Langevin dynamics at 300 K temperature. The MD simulations were performed with a flexible cell size and constant ratio of 1:1 for the *x*- and *y*-dimensions to stabilize the membrane that has been placed in the plane. MD simulations were performed without adding explicit ions to the solution.

2.2. Atomic partial charges of CcO cofactors

Atomic partial charges of the cofactors were calculated as in [12] and earlier applications [39], with the quantum chemical program Jaguar v.7.7 [40] using the B3LYP DFT functional and LACVP** basis set. A similar method was also used by Johansson et al. [41]. The cofactor geometries were optimized quantum chemically in two steps: (i) optimizing hydrogen atoms and BNC ligands (neutral and deprotonated waters), which was done for heme a_3 and Cu_B simultaneously; (ii) optimizing all atoms for each cofactor separately (heme *a*, heme a_3, Cu_A, Cu_B, including the corresponding ligands), while constraining torsion angles. In the second optimization step (ii), the following distances were also constrained: (a) Cu_B-oxygen distance to 2.14 Å (obtained in the first optimization step (i), including heme a_3) in the charge states Cu(II)-OH/Tyr237$^-$ and Cu(II)-OH/Tyr237*, (b) the Fe-oxygen distance for heme a_3 to 2.27 Å (obtained in the first optimization step (i), including the Cu_B complex) in state Fe(II)-H_2O, and (c) copper-sulfur distance of the dimethyl-sulfide ligand to 2.47 Å in the Cu_A complex (corresponding to the crystal structure). Then, the electrostatic potentials in the vicinity of the cofactors were computed based on the electronic wave functions and charges of the nuclei using the same procedure as for geometry optimization. Atomic partial charges of the cofactors were determined based on these electrostatic potentials, employing a two-stage restraint-electrostatic-potential (RESP) [42,43] procedure. The Cu_B center calculation included Tyr288 being covalently bound to His284. The resulting coordinates and atomic partial charges are given in Table S4 of Supporting Information.

2.3. Computation of pK_A values

pK_A values were evaluated by electrostatic energy computations using Karlsberg+ [44,45], as done previously for CcO [12]. Karlsberg+ was applied for the crystal structure and alternatively for time frames from MD simulations taken every 100 ps. Except for one test calculation, crystal water molecules were removed. The resulting cavity volumes and the bulk solvent were represented by a dielectric continuum of $\varepsilon = 80$. Membrane molecules were not considered explicitly. However, within a 20 Å sphere around Lys362 the lipids were represented by a dielectric continuum of 4. Outside of the protein and the membrane slap, the dielectric constant was set to 80. Such conditions were tested and used before under similar conditions [12]. An implicit ion concentration of 100 mM was included in the calculations.

3. Results and discussion

3.1. Molecular dynamics simulation

The two-subunit CcO from *R. sphaeroides* [Protein Data Bank (PDB) id 2GSM [17]] was embedded in a phosphatidylcholine membrane. All redox states and intermediate states were investigated, except state A where O_2-binding occurs (Fig. 1). Details of the chemistry of the intermediate states inside the BNC are not known with certainty. In this work, we propose that the electron will enter the BNC before the chemical proton and drag chemical and pumped protons (located as shown in Fig. 1). The resulting redox states of the BNC agree with the current view of Wikström and coworkers [1,3,5], except for the $P_M \rightarrow F$ transition (see Fig. 1). We believe that the P_R state observed under non-physiological conditions is replaced by the transient $P \rightarrow F$ state as discussed below.

The protonation state of all residues was determined with a pK_A calculation based on the crystal structure (PDB id 2GSM [17]) using implicit water. The histidine protonations (involving 28 histidines) are given in Table S1 of Supporting Information. All other titratable groups (Asp, Glu, Arg and Lys) are always charged except the charge neutral Asp407 and Glu286, while the charge of Lys362 is variable. This protonation pattern was applied for all MD runs, varying only the chemistry inside the BNC (including Tyr288) and the protonation state of Lys362. In this study, we observe that the protonated Lys362 moves upward closer to BNC and Tyr288 (Fig. 2B) for most of the considered BNC redox states displayed in Fig. 1. An example for an upward conformation of Lys362 obtained from MD is shown in Fig. 2A, together with the Lys362 conformation in the crystal structure.

Lys362 does not move in a discrete flipping event between two states since the torsion angles of its side chain change continuously during the MD simulation. Along with the motion of Lys362, the K-channel widens slightly and helix VII and helix VIII move apart by 2.6 Å (Table S2 of Supporting Information), as seen by the increasing distances between the corresponding backbone atoms. This is in line with the work of Ferguson-Miller and coworkers [46–48], who observed structural differences between reduced and oxidized CcO crystals specifically in helix VIII and the farnesyl tail of heme a_3. In a computational analysis, they found that the protein backbone lining the K-channel is more flexible than other parts of CcO [46]. In addition, Armstrong and coworkers detected that the residues surrounding Lys362 are accessible to deuterium exchange in the R state at the end of the reductive half, but have limited or no access in the oxidative half (P_M, F and O state) of the reaction cycle [49].

The water content of the K-channel has been largely debated [28,29,47], as in the crystal structures, there are only a few disconnected water molecules [17]. Chakrabarty and Warshel recently demonstrated the importance of the correct number of water molecules surrounding a titratable residue, also specifically for CcO [50]. In MD simulations with protonated Lys362, water molecules enter CcO, move into the K-channel and widen it. Typically within the first nanosecond of MD simulation, the charged head group of Lys362 becomes embedded in a water shell, which is stable until the end of the MD simulation (see Fig. S2 of Supporting Information). At the same time Lys362 forms an H-bond network with Tyr288 via two or three water molecules eventually also connecting to Thr359. Only in the redox states E_H and R, where Tyr288 is protonated, Lys362 loses its H-bond contact with Tyr288 and thus with the BNC ligands during MD simulations of several nanoseconds.

In MD simulations, the side chain conformations of deprotonated Lys362 are very similar to the crystal structure. The deprotonated Lys362 rarely moves upwards and, when it does, it returns after 200 ps at most. In the P_M, O and the intermediate $E \rightarrow R$ state, the deprotonated Lys362 moves upwards four, one and three times, respectively. Only in the $O \rightarrow E$ intermediate state the deprotonated Lys362 moves upwards more often and stays there for about one-third of the time in a 10 ns MD simulation. For deprotonated Lys362, no water molecules are moving inside the K-channel, whose geometry remains essentially invariant (Fig. 2B and Table S2 of Supporting Information). Thus, our MD simulations indicate that only protonated Lys362 is capable of bridging the gap to Tyr288, rendering the K-channel proton-conductive. To further explore this possibility, we computed the pK_A of Lys362 in the different redox states.

3.2. pK_A value of Lys362

Based on the crystal structure and modeling of the charge pattern of the redox state chemistry inside the BNC, pK_A values for Lys362 were

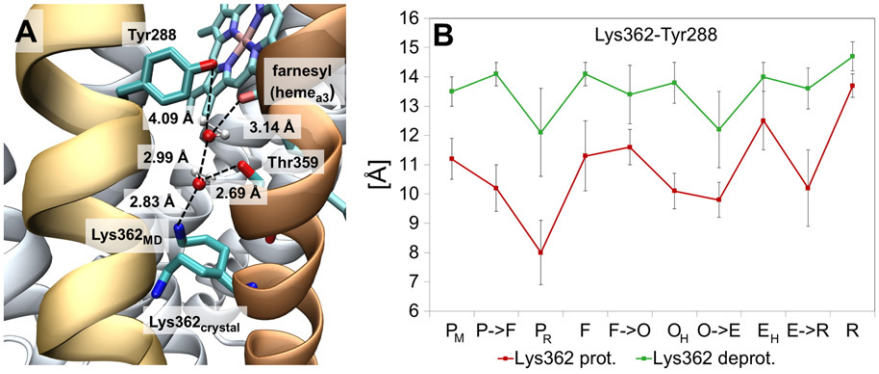

Fig. 2. Protonated Lys362 moves upwards to the BNC. (A) Part of CcO crystal structure (PDB id 2GSM [17]) with Lys362 (pointing downwards). The second displayed Lys362 conformation (pointing upwards) is taken from a representative MD snapshot of the intermediate state $O \rightarrow E$ (Fig. 1) after 9.3 ns of MD simulation. The two water molecules are also taken from the same MD snapshot. Their H-bond distances are given in angstroms. Backbone coordinates are taken from the crystal structure; helix VII is shown in yellow and helix VIII in orange. The positions of all residues and cofactors of the displayed crystal structure differ only marginally from the aligned structure of the considered MD snapshot. (B) Mean distance between nitrogen of Lys362 and oxygen of Tyr288 side chain in MD simulation. Error bars indicate standard deviation. The corresponding distance in the crystal structure is 13.8 Å.

calculated by continuum electrostatics as explained in Methods. In agreement with most previous studies [18,19], the computed pK_A value of Lys362 is below zero, when based on the geometry of the C*c*O crystal structure, regardless of the BNC redox state (Table 1). Computations with explicit water yield similar results (Table S3 of Supporting Information). However, pK_A calculations with explicit water are very sensitive to details of modeling, which may explain differences with other approaches [20].

To take alternative protein conformations into account, the pK_A value of Lys362 was also calculated from MD simulation time frames. While MD simulations with deprotonated Lys362 lead to lower pK_A values, those with protonated Lys362 lead to higher pK_A values (Table 1), since the respective protonation state has a tendency to be stabilized in the corresponding MD simulation. Also, a significant difference in pK_A was observed depending on the BNC redox state. According to these calculations, Lys362 is deprotonated in the ground states (P_M, F, E_H, O_H and R; inner cycle of Fig. 1), but may become transiently protonated in the intermediate states (outer cycle of Fig. 1), thereby rendering the K-channel proton-conductive. The P_R state (Fig. 1), which is detected after dioxygen splitting under non-physiological highly reduced conditions, is also considered. P_R formation is slowed down for mutants blocking K-channel function, in contrast to both P_M and F formation being unchanged [24]. However, for the physiological C*c*O reaction cycle, delivery of the chemical proton follows the formation of intermediate states (Fig. 1). Thus, in the following, we focus on these intermediate states in more detail.

We calculated the pK_A variation of Lys362 as a function of time in the four intermediate states (non-dashed outer circles in Fig. 1) using time frames of 50 ns MD trajectories simulated with protonated Lys362 (Fig. 3). For the O → E intermediate and even more pronounced for the E → R intermediate, the pK_A rises strongly in the beginning of the MD simulation to values above ten and higher. Subsequently, the pK_A drops back to lower values and slowly rises again. In contrast, the pK_A of the F → O intermediate remains low and rarely rises above seven. In the P → F intermediate, the pK_A of Lys362 remains low in the beginning as in the F → O intermediate, but rises slowly later in the MD simulation (Fig. 3).

We analyzed the factors that cause these variations in Lys362 pK_A with the redox state of the BNC in more detail in the following. The Lys362–Tyr288 distance is similar in MD simulations of all intermediate states with protonated Lys362 (Fig. 2B), only slightly larger in the P → F and shorter in the P_R state. In all MD simulations, a water shell is formed around the protonated Lys362. A direct electrostatic effect of the BNC redox state on Lys362 was tested using time frames of the O → E intermediate MD simulation for pK_A computations with charge patterns corresponding to the BNC redox states of all other intermediate states (Fig. 4). Accordingly, Lys362 shows pK_A values that are larger by about 2.3 pH units in the O → E and E → R than in the P → F and F → O intermediate states. Therefore, the pK_A difference observed between reductive phase intermediates (O → E and E → R) and oxidative phase intermediates (P → F and F → O; Table 1 and Fig. 3) is mainly caused by the direct electrostatic interaction of Lys362 with the BNC. From this observation, we may deduce a simple model of K-channel regulation in C*c*O; i.e. the K-channel opens in the reductive phase and closes in the oxidative phase via changes in the BNC charge pattern facilitating Lys362 to protonate and change its conformation. Thus, Lys362 regulates proton access to the BNC via the K-channel.

Table 1
Computed Lys362 pK_A values for all redox states of C*c*O as depicted in Fig. 1, based on crystal structure and averages of time frames from MD simulations with protonated and deprotonated Lys362. Standard deviation is given in parentheses. The pK_A values are averaged over 100 time frames from MD simulations of a total length of 10 ns. The computation of pK_A values was performed with Karlsberg+ [44,45] as described in Methods.

Redox state	Crystal structure	MD K362 protonated	MD K362 deprotonated
P_M	−3	3.0 (2.0)	−4.3 (1.5)
P → F	−1.6	4.6 (2.1)	−3.2 (1.8)
P_R	−0.9	7.6 (2.0)	−2.5 (1.5)
F	−2.2	3.9 (2.0)	−4.5 (1.2)
F → O	−1.6	4.4 (1.7)	−3.5 (1.6)
O_H	−2.9	4.3 (2.1)	−4.8 (1.6)
O → E	−0.3	6.5 (2.9)	−1.4 (1.5)
E_H	−2.8	5.9 (2.5)	−5.8 (2.0)
E → R	−0.3	7.8 (2.3)	−2.6 (1.7)
R	−2.7	2.3 (1.8)	−4.2 (1.3)

3.3. Comparison with experimental data

Our results obtained in this study agree and provide insight into several experimental observations. The upward movement of Lys362 suggested by several experimentalists [24–26] has been shown here explicitly by MD simulation. Also, the fact that the residues lining the K-channel have increased flexibility [46] and changed their positions [47,48] and accessibility [49] upon opening and closing of the K-channel was very well reproduced in the present MD simulation studies.

In accordance with experiments [24–26,51], Lys362 is protonated in the P_R state (Table 1). The P_R state is detected after dioxygen splitting under non-physiological highly reduced conditions [4], where C*c*O carries one additional electron inside the BNC as compared to the P_M state. We propose that the P_M → F transition does not necessarily occur via the P_R state but by an alternative P → F intermediate state. In many works, P_R state and P → F intermediates are considered to be identical. We assume that the electron entering the BNC in the P_M state stays transiently at heme a_3 (constituting the P → F intermediate state) until a protonation step leads to state F. A transient trapping of the electron at heme a_3 could potentially be supported by protonation of the PLS, although the nature of the PLS is not yet known. However, even under physiological conditions, the P_R state may follow the P → F transiently. We assume, however, that the chemical proton will promptly enter the BNC from the D-channel to form state F, leaving no time for Lys362 to become protonated and open the K-channel. This scenario is hard to prove experimentally, but several findings are in line with it. It was shown that the P_R state of the fully reduced C*c*O probably does not form via the P_M state [4], but that under the conditions of P_R state formation, one electron for oxygen splitting is delivered by heme *a* and not by Tyr288, which forms an anion and not a radical as in the P_M state (Fig. 1). Vice versa, it may be speculated that adding one electron to the P_M state only leads to P_R formation via a P → F intermediate having the electron on heme a_3. Additionally, quantum chemical calculations revealed the P_M to P_R transition to be slightly endergonic, while the P_R to F transition is strongly exergonic [3], which indicates a short life-time for the P_R state if it is occupied transiently under physiological conditions.

It is reasonable to assume that each step of the reaction cycle begins with an electron entering the BNC (denoted by the intermediate states in Fig. 1) before a chemical proton is accepted [1,3,5]. In addition, it was shown experimentally that one electron is trapped inside the BNC in the O → E intermediate state when the K-channel is blocked by the Lys362Met mutant [22]. This electron was observed to be evenly distributed over Cu_B and heme a_3 [22]. Thus, it is likely located on Cu_B for a certain period of time or it might reach Cu_B in a concerted reaction with the protonation of Lys362 in wild type C*c*O.

We expect the protonation of Lys362 to be the rate-limiting step in proton delivery via the K-channel. At high pH, proton delivery is indeed rate-limiting [23], which may be explained by Lys362 remaining deprotonated under these conditions. The transition of E → R is faster than of O → E [21]. This difference in the two reaction rates may be due to the pK_A increase of Lys362 from O → E to E → R intermediates (Fig. 3).

With our calculations, we have demonstrated that the sum of charges of the Cu_B center, including Tyr288, must be negative or charge-neutral for Lys362 to become protonated and move towards the BNC. Based on our quantum chemically computed BNC charge pattern,

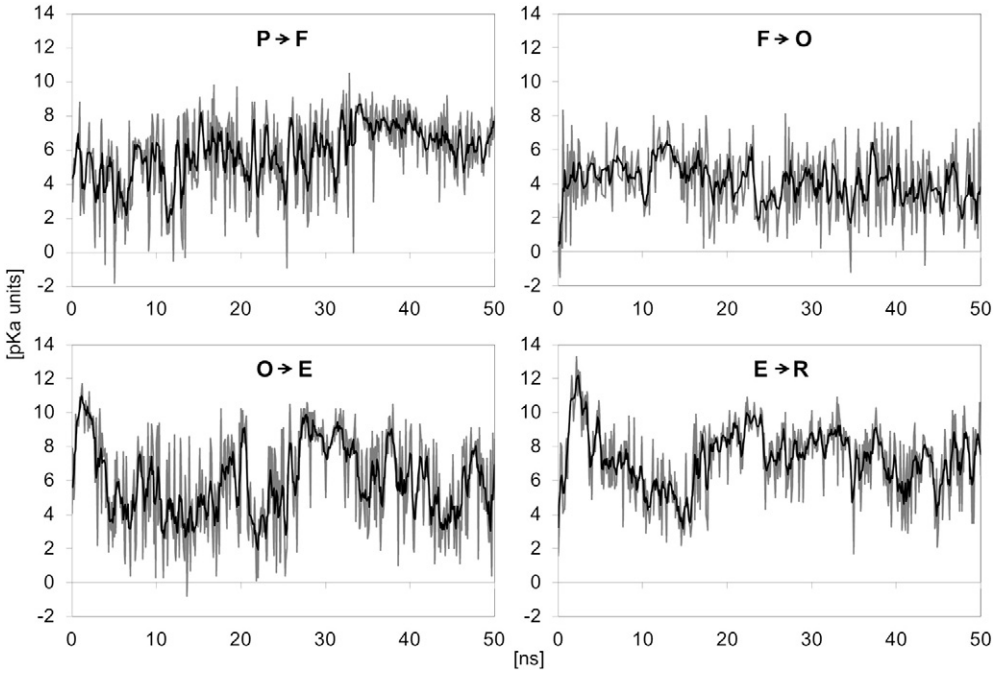

Fig. 3. Time dependence of the pK_A values of protonated Lys362 for the four intermediate states (see Fig. 1) in the catalytic cycle of C*c*O. Results of MD time frames are shown in steps of 100 ps (gray curve). Averages of five subsequent time frames are also shown (black curve). All other protonation states are as described in the main text. The pK_A computation was performed with Karlsberg+ [44,45] as described in Methods.

this occurs in the intermediate states O → E and E → R as well as in the P_R state, but not in the P → F and F → O intermediates (for a definition of states, see Fig. 1). These observations allow the development of a model explaining the access of chemical protons to the BNC. Accordingly, the opening of the K-channel is regulated by pK_A and the conformation of Lys362, which itself depends predominantly on the charge of the Cu_B center including Tyr288.

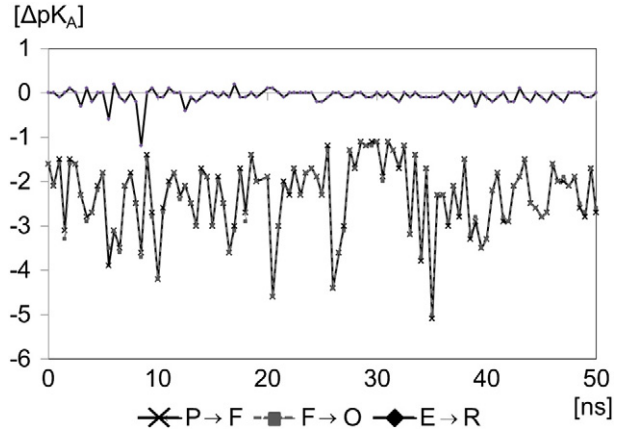

Fig. 4. Differences in Lys362 pK_A values (ΔpK_A) for different BNC redox states. Geometries were taken from 100 time frames of MD simulation in steps of 100 ps generated for the O → E intermediate state. The pK_A computations were performed with Karlsberg+ [44,45] adapting the charge pattern of the BNC to different redox states (P → F, F → O, E → R). pK_A values obtained for the redox state (O → E)—for which the MD trajectory was generated—were subtracted from the pK_A values obtained with the BNC charge pattern belonging to the other three intermediate states. The charge pattern for the O → E intermediate is similar to that of the E → R intermediate both having the additional electron localized on the Cu_B center (see Fig. 1). In contrast, the P → F and F → O intermediates carry the additional electron on heme a_3. Since the O → E simulation serves as a reference and resembles the E → R state, the E → R pK_A differences are close to zero and fluctuate less than the pK_A differences for the P → F and F → O transition.

4. Conclusion

In this study, we systematically investigated conformations and pK_A values of Lys362 within the K-channel of C*c*O for the different BNC redox states. Most importantly, we found a strong correlation between conformational change and pK_A increase of Lys362 and the BNC charge pattern in the reductive half of the catalytic C*c*O cycle. MD simulations show that protonated Lys362 may move upwards and bridge the gap to Tyr288 via an H-bond chain involving water. From pK_A calculations, we found that the protonation probability of Lys362 increases with the reduction of the BNC. For the actual protonation of Lys362, three prerequisites are needed: (i) uncompensated electron charge in the BNC, (ii) reduced Cu_B and (iii) deprotonated Tyr288. Based on these results, we developed a model for the mechanism of K-channel opening and closing, which can interpret experimental facts that have thus far remained unexplained. Similar to the role of Glu286 in gating chemical and pumped protons of the D-channel, our model assigns a key role to Lys362 for proton gating of the K-channel of C*c*O.

In this context, it is interesting to note that only the A-type C*c*O switches between two proton input channels, while the B- and C-type C*c*O use only one K-analogue proton input channel, which also ends at Tyr288, but has an continuous hydrogen bonding network without lysine [52,53]. Therefore, it is reasonable to assume that the A-type K-channel must have a closing mechanism to prevent proton conductance during the whole catalytic cycle. Our model assigns this closing mechanism to Lys362. This model can be a valuable starting point for testing its consequences experimentally and refining the model with further experimental knowledge. This could be a key step toward understanding how A-type C*c*O regulates its two proton channels.

Acknowledgement

We gratefully acknowledge financial support from the Deutsche Forschungsgemeinschaft (DFG) in the frame of the collaborative research center (CRC) 1078, project C2 and the research training group "Computational System Biology" (CSB).

Appendix A. Supplementary data

Supplementary data to this article can be found online at http://dx.doi.org/10.1016/j.bbabio.2014.08.003.

References

[1] V.R. Kaila, M.I. Verkhovsky, M. Wikstrom, Proton-coupled electron transfer in cytochrome oxidase, Chem. Rev. 110 (2010) 7062–7081.
[2] P. Brzezinski, R.B. Gennis, Cytochrome *c* oxidase: exciting progress and remaining mysteries, J. Bioenerg. Biomembr. 40 (2008) 521–531.
[3] V.R. Kaila, M.P. Johansson, D. Sundholm, L. Laakkonen, M. Wistrom, The chemistry of the CuB site in cytochrome *c* oxidase and the importance of its unique His-Tyr bond, Biochim. Biophys. Acta 1787 (2009) 221–233.
[4] J.E. Morgan, M.I. Verkhovsky, G. Palmer, M. Wikstrom, Role of the PR intermediate in the reaction of cytochrome *c* oxidase with O_2, Biochemistry 40 (2001) 6882–6892.
[5] V. Sharma, K.D. Karlin, M. Wikstrom, Computational study of the activated O(H) state in the catalytic mechanism of cytochrome c oxidase, Proc. Natl. Acad. Sci. U. S. A. 110 (2013) 16844–16849.
[6] S. Junemann, B. Meunier, R.B. Gennis, P.R. Rich, Effects of mutation of the conserved lysine-362 in cytochrome c oxidase from *Rhodobacter sphaeroides*, Biochemistry 36 (1997) 14456–14464.
[7] A.A. Konstantinov, S. Siletsky, D. Mitchell, A. Kaulen, R.B. Gennis, The roles of the two proton input channels in cytochrome c oxidase from *Rhodobacter sphaeroides* probed by the effects of site-directed mutations on time-resolved electrogenic intraprotein proton transfer, Proc. Natl. Acad. Sci. U. S. A. 94 (1997) 9085–9090.
[8] P. Adelroth, R.B. Gennis, P. Brzezinski, Role of the pathway through K(I-362) in proton transfer in cytochrome c oxidase from *R. sphaeroides*, Biochemistry 37 (1998) 2470–2476.
[9] T.V. Vygodina, C. Pecoraro, D. Mitchell, R. Gennis, A.A. Konstantinov, Mechanism of inhibition of electron transfer by amino acid replacement K362M in a proton channel of *Rhodobacter sphaeroides* cytochrome c oxidase, Biochemistry 37 (1998) 3053–3061.
[10] M.R.A. Blomberg, P.E.M. Siegbahn, Proton pumping in cytochrome c oxidase: energetic requirements and the role of two proton channels, Biochim. Biophys. Acta 1837 (7) (2014) 1165–1177.
[11] M.A. Sharpe, S. Ferguson-Miller, A chemically explicit model for the mechanism of proton pumping in heme-copper oxidases, J. Bioenerg. Biomembr. 40 (2008) 541–549.
[12] A.L. Woelke, G. Galstyan, A. Galstyan, T. Meyer, J. Heberle, E.W. Knapp, Exploring the possible role of Glu286 in CcO by electrostatic energy computations combined with molecular dynamics, J. Phys. Chem. B 117 (2013) 12432–12441.
[13] D.M. Popovic, A.A. Stuchebrukhov, Coupled electron and proton transfer reactions during the O → E transition in bovine cytochrome c oxidase, Biochim. Biophys. Acta 1817 (2012) 506–517.
[14] S. Chakrabarty, I. Namslauer, P. Brzezinski, A. Warshel, Exploration of the cytochrome c oxidase pathway puzzle and examination of the origin of elusive mutational effects, Biochim. Biophys. Acta 1807 (2011) 413–426.
[15] A.L. Johansson, S. Chakrabarty, C.L. Berthold, M. Hogbom, A. Warshel, P. Brzezinski, Proton-transport mechanisms in cytochrome c oxidase revealed by studies of kinetic isotope effects, Biochim. Biophys. Acta 1807 (2011) 1083–1094.
[16] C. Ostermeier, A. Harrenga, U. Ermler, H. Michel, Structure at 2.7 A resolution of the *Paracoccus denitrificans* two-subunit cytochrome c oxidase complexed with an antibody FV fragment, Proc. Natl. Acad. Sci. U. S. A. 94 (1997) 10547–10553.
[17] L. Qin, C. Hiser, A. Mulichak, R.M. Garavito, S. Ferguson-Miller, Identification of conserved lipid/detergent-binding sites in a high-resolution structure of the membrane protein cytochrome c oxidase, Proc. Natl. Acad. Sci. U. S. A. 103 (2006) 16117–16122.
[18] A. Kannt, C.R. Lancaster, H. Michel, The coupling of electron transfer and proton translocation: electrostatic calculations on *Paracoccus denitrificans* cytochrome c oxidase, Biophys. J. 74 (1998) 708–721.
[19] Y. Song, E. Michonova-Alexova, M.R. Gunner, Calculated proton uptake on anaerobic reduction of cytochrome c oxidase: is the reaction electroneutral? Biochemistry 45 (2006) 7959–7975.
[20] A. Tuukkanen, M.I. Verkhovsky, L. Laakkonen, M. Wikstrom, The K-pathway revisited: a computational study on cytochrome c oxidase, Biochim. Biophys. Acta 1757 (2006) 1117–1121.
[21] M.I. Verkhovsky, A. Tuukkanen, C. Backgren, A. Puustinen, M. Wikstrom, Charge translocation coupled to electron injection into oxidized cytochrome c oxidase from *Paracoccus denitrificans*, Biochemistry 40 (2001) 7077–7083.
[22] K. Ganesan, R.B. Gennis, Blocking the K-pathway still allows rapid one-electron reduction of the binuclear center during the anaerobic reduction of the aa3-type cytochrome c oxidase from *Rhodobacter sphaeroides*, Biochim. Biophys. Acta 1797 (2010) 619–624.
[23] D. Riegler, L. Shroyer, C. Pokalsky, D. Zaslavsky, R. Gennis, L.J. Prochaska, Characterization of steady-state activities of cytochrome c oxidase at alkaline pH: mimicking the effect of K-channel mutations in the bovine enzyme, Biochim. Biophys. Acta 1706 (2005) 126–133.
[24] M. Branden, H. Sigurdson, A. Namslauer, R.B. Gennis, P. Adelroth, P. Brzezinski, On the role of the K-proton transfer pathway in cytochrome c oxidase, Proc. Natl. Acad. Sci. U. S. A. 98 (2001) 5013–5018.
[25] M. Branden, F. Tomson, R.B. Gennis, P. Brzezinski, The entry point of the K-proton-transfer pathway in cytochrome c oxidase, Biochemistry 41 (2002) 10794–10798.
[26] H. Lepp, E. Svahn, K. Faxen, P. Brzezinski, Charge transfer in the K proton pathway linked to electron transfer to the catalytic site in cytochrome c oxidase, Biochemistry 47 (2008) 4929–4935.
[27] I. Hofacker, K. Schulten, Oxygen and proton pathways in cytochrome c oxidase, Proteins 30 (1998) 100–107.
[28] E. Olkhova, M.C. Hutter, M.A. Lill, V. Helms, H. Michel, Dynamic water networks in cytochrome c oxidase from *Paracoccus denitrificans* investigated by molecular dynamics simulations, Biophys. J. 86 (2004) 1873–1889.
[29] R.I. Cukier, A molecular dynamics study of water chain formation in the proton-conducting K channel of cytochrome c oxidase, Biochim. Biophys. Acta 1706 (2005) 134–146.
[30] A. Warshel, S.T. Russell, Calculations of electrostatic interactions in biological systems and in solutions, Q. Rev. Biophys. 17 (1984) 283–422.
[31] V.R. Kaila, M.I. Verkhovsky, G. Hummer, M. Wikstrom, Glutamic acid 242 is a valve in the proton pump of cytochrome c oxidase, Proc. Natl. Acad. Sci. U. S. A. 105 (2008) 6255–6259.
[32] H.M. Berman, J. Westbrook, Z. Feng, G. Gilliland, T.N. Bhat, H. Weissig, I.N. Shindyalov, P.E. Bourne, The Protein Data Bank, Nucleic Acids Res. 28 (2000) 235–242.
[33] G. Gilderson, L. Salomonsson, A. Aagaard, J. Gray, P. Brzezinski, J. Hosler, Subunit III of cytochrome c oxidase of *Rhodobacter sphaeroides* is required to maintain rapid proton uptake through the D pathway at physiologic pH, Biochemistry 42 (2003) 7400–7409.
[34] W. Humphrey, A. Dalke, K. Schulten, VMD: visual molecular dynamics, J. Mol. Graph. 14 (1996) 33–38 (27–38).
[35] W.L. Jorgensen, J. Chandrasekhar, J.D. Madura, R.W. Impey, M.L. Klein, Comparison of simple potential functions for simulating liquid water, J. Chem. Phys. 79 (1983) 926–935.
[36] B.R. Brooks, C.L. Brooks III, A.D. Mackerell Jr., L. Nilsson, R.J. Petrella, B. Roux, Y. Won, G. Archontis, C. Bartels, S. Boresch, A. Caflisch, L. Caves, Q. Cui, A.R. Dinner, M. Feig, S. Fischer, J. Gao, M. Hodoscek, W. Im, K. Kuczera, T. Lazaridis, J. Ma, V. Ovchinnikov, E. Paci, R.W. Pastor, C.B. Post, J.Z. Pu, M. Schaefer, B. Tidor, R.M. Venable, H.L. Woodcock, X. Wu, W. Yang, D.M. York, M. Karplus, CHARMM: the biomolecular simulation program, J. Comput. Chem. 30 (2009) 1545–1614.
[37] J.B. Klauda, R.M. Venable, J.A. Freites, J.W. O'Connor, D.J. Tobias, C. Mondragon-Ramirez, I. Vorobyov, A.D. MacKerell Jr., R.W. Pastor, Update of the CHARMM all-atom additive force field for lipids: validation on six lipid types, J. Phys. Chem. B 114 (2010) 7830–7843.
[38] J.C. Phillips, R. Braun, W. Wang, J. Gumbart, E. Tajkhorshid, E. Villa, C. Chipot, R.D. Skeel, L. Kale, K. Schulten, Scalable molecular dynamics with NAMD, J. Comput. Chem. 26 (2005) 1781–1802.
[39] H. Ishikita, E.W. Knapp, Redox potential of quinones in both electron transfer branches of photosystem I, J. Biol. Chem. 278 (2003) 52002–52011.
[40] Jaguar, Version 7.7, Schrödinger, LLC, New York, NY, 2010.
[41] M.P. Johansson, V.R. Kaila, L. Laakkonen, Charge parameterization of the metal centers in cytochrome c oxidase, J. Comput. Chem. 29 (2008) 753–767.
[42] C.I. Bayly, P. Cieplak, W.D. Cornell, P.A. Kollman, A well-behaved electrostatic potential based method using charge restraints for deriving atomic charges—the RESP model, J. Phys. Chem. 97 (1993) 10269–10280.
[43] W.D. Cornell, P. Cieplak, C.I. Bayly, P.A. Kollman, Application of RESP charges to calculate conformational energies, hydrogen-bond energies, and free-energies of solvation, J. Am. Chem. Soc. 115 (1993) 9620–9631.
[44] B. Rabenstein, E.W. Knapp, Calculated pH-dependent population and protonation of carbon-monoxy-myoglobin conformers, Biophys. J. 80 (2001) 1141–1150.
[45] G. Kieseritzky, E.W. Knapp, Optimizing pKa computation in proteins with pH adapted conformations, Proteins 71 (2008) 1335–1348.
[46] L. Buhrow, S. Ferguson-Miller, L.A. Kuhn, From static structure to living protein: computational analysis of cytochrome c oxidase main-chain flexibility, Biophys. J. 102 (2012) 2158–2166.
[47] J. Liu, L. Qin, S. Ferguson-Miller, Crystallographic and online spectral evidence for role of conformational change and conserved water in cytochrome oxidase proton pump, Proc. Natl. Acad. Sci. U. S. A. 108 (2011) 1284–1289.
[48] L. Qin, J. Liu, D.A. Mills, D.A. Proshlyakov, C. Hiser, S. Ferguson-Miller, Redox-dependent conformational changes in cytochrome c oxidase suggest a gating mechanism for proton uptake, Biochemistry 48 (2009) 5121–5130.
[49] L.S. Busenlehner, L. Salomonsson, P. Brzezinski, R.N. Armstrong, Mapping protein dynamics in catalytic intermediates of the redox-driven proton pump cytochrome c oxidase, Proc. Natl. Acad. Sci. U. S. A. 103 (2006) 15398–15403.
[50] S. Chakrabarty, A. Warshel, Capturing the energetics of water insertion in biological systems: the water flooding approach, Proteins 81 (2013) 93–106.
[51] M. Rintanen, I. Belevich, M.I. Verkhovsky, Electrogenic events upon photolysis of CO from fully reduced cytochrome c oxidase, Biochim. Biophys. Acta 1817 (2012) 269–275.
[52] H.Y. Chang, J. Hemp, Y. Chen, J.A. Fee, R.B. Gennis, The cytochrome ba3 oxygen reductase from *Thermus thermophilus* uses a single input channel for proton delivery to the active site and for proton pumping, Proc. Natl. Acad. Sci. U. S. A. 106 (2009) 16169–16173.
[53] V. Rauhamaki, D.A. Bloch, M. Wikstrom, Mechanistic stoichiometry of proton translocation by cytochrome cbb3, Proc. Natl. Acad. Sci. U. S. A. 109 (2012) 7286–7291.